

# RoCo-Sim: Enhancing Roadside Collaborative Perception through Foreground Simulation

Yuwen Du<sup>1,2\*</sup> Anning Hu<sup>1\*</sup> Zichen Chao<sup>3</sup> Yifan Lu<sup>1</sup> Junhao Ge<sup>1</sup> Genjia Liu<sup>1</sup>  
 Weitao Wu<sup>3</sup> Lanjun Wang<sup>2</sup> Siheng Chen<sup>1†</sup>

<sup>1</sup> Shanghai Jiao Tong University <sup>2</sup> Tianjin University <sup>3</sup> Nanjing University of Science and Technology  
 {huanning, yifan\_lu, cancaries, LGJ1zed, sihengc}@sjtu.edu.cn  
 {duyuwen, wanglanjun}@tju.edu.cn, {zichen.chao, weitaowwtw}@njjust.edu.cn

## Abstract

Roadside Collaborative Perception refers to a system where multiple roadside units collaborate to pool their perceptual data, assisting vehicles in enhancing their environmental awareness. Existing roadside perception methods concentrate on model design but overlook data issues like calibration errors, sparse information, and multi-view consistency, leading to poor performance on recent published datasets. To significantly enhance roadside collaborative perception and address critical data issues, we present the first simulation framework RoCo-Sim for roadside collaborative perception. RoCo-Sim is capable of generating diverse, multi-view consistent simulated roadside data through dynamic foreground editing and full-scene style transfer of a single image. RoCo-Sim consists of four components: (1) Camera Extrinsic Optimization ensures accurate 3D to 2D projection for roadside cameras; (2) A novel Multi-View Occlusion-Aware Sampler (MOAS) determines the placement of diverse digital assets within 3D space; (3) DepthSAM innovatively models foreground-background relationships from single-frame fixed-view images, ensuring multi-view consistency of foreground; and (4) Scalable Post-Processing Toolkit generates more realistic and enriched scenes through style transfer and other enhancements. RoCo-Sim significantly improves roadside 3D object detection, outperforming SOTA methods by **83.74%** on Rcooper-Intersection and **83.12%** on TUMTraf-V2X for AP70. RoCo-Sim fills a critical gap in roadside perception simulation. Code and pre-trained models will be released soon: <https://github.com/duyuwen-duen/RoCo-Sim>

## 1. Introduction

Roadside Collaborative Perception [23, 25, 29, 40] is a cooperative system that integrates perceptual data from

\*Equal contribution.

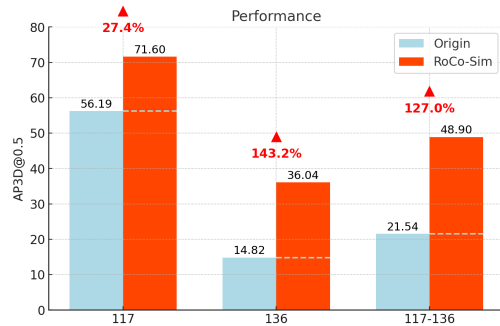


Figure 1. **Performance on RCooper-Intersection[8], 117 and 136.** With RoCo-Sim, camera-only 3D detection model BEVHeight [40] achieves significantly better performance.

multiple roadside units to help vehicles improve their understanding of the surrounding environment. This system serves as an effective supplement to autonomous driving, enhancing vehicle safety by addressing blind spots and providing a more comprehensive view of the road conditions. In Roadside Collaborative Perception, camera-based systems play a pivotal role by capturing rich visual information that can be leveraged to infer detailed 3D environmental characteristics. However, current methods utilizing camera-only systems for 3D detection in roadside collaborative perception have not yet achieved optimal results.

Existing roadside perception methods [16, 23, 25, 29], primarily focus on designing model architectures that aim to capture more information from the available data. However, these methods often overlook data issues. Firstly, the extrinsics of fixed-view cameras are difficult to calibrate initially and tend to drift over time due to environmental factors like mounting shifts or external interference, requiring frequent recalibration. Secondly, during data collection, long periods with few or no vehicles in the field of view result in sparse information density. Thirdly, ensuring multi-view consistency in annotations is highly challenging, leading to low-quality labeled data and high data collection costs. These

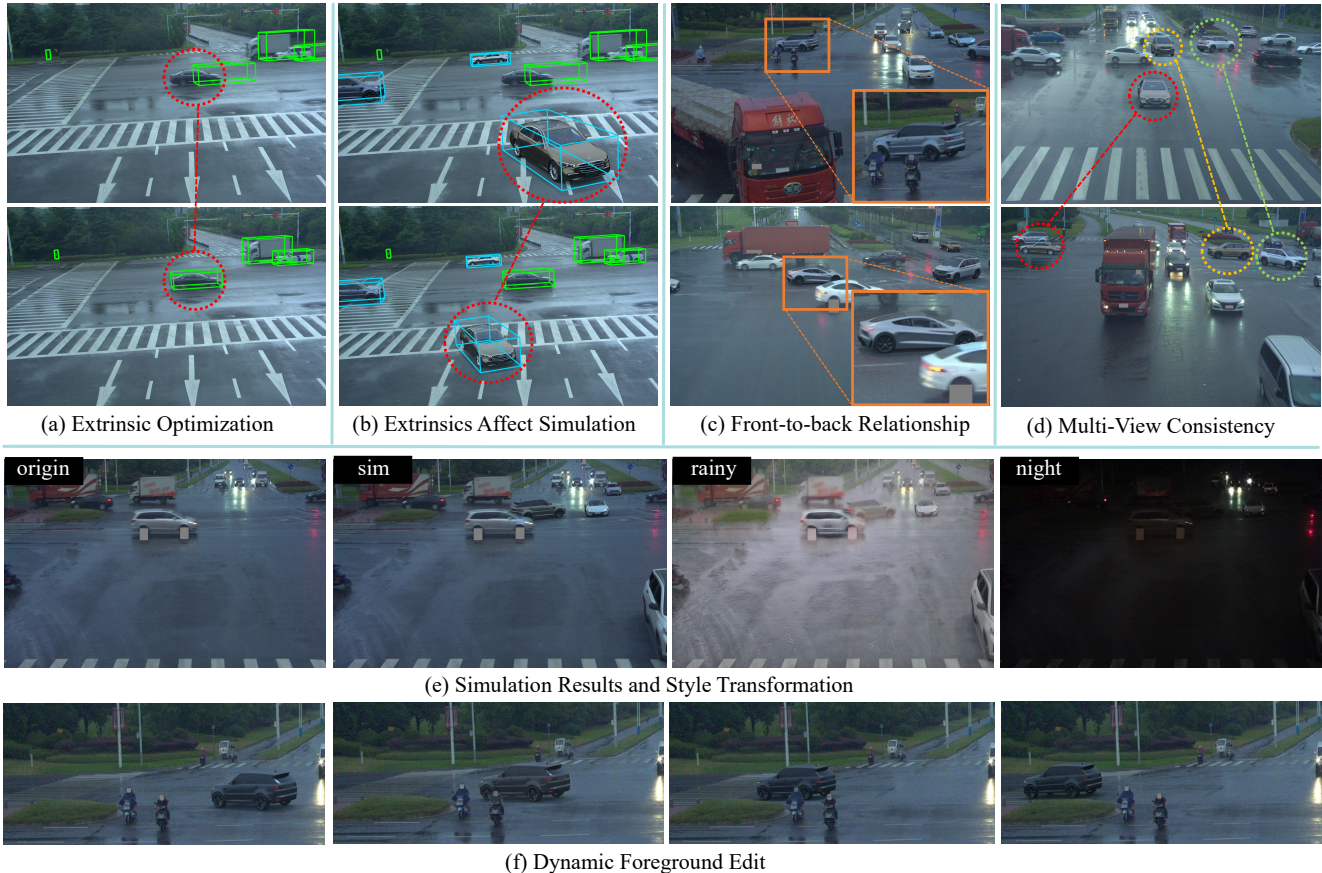


Figure 2. (a) After extrinsic optimization, the projection of 3D bounding boxes is more accurate. (b) Camera extrinsic calibration can ensure the correct imaging of simulated objects, reducing the gap between simulated and real objects. (c) DepthSAM allows 3D simulated objects to be rendered onto 2D images while preserving the front-to-back relationships between objects. (d) Roco-Sim simulation can ensure multi-view consistency. (e) Roco-Sim can generate realistic and diverse simulated scenes. “origin” refers to the original image, and “sim” depicts the simulation of 4 cars. Furthermore, with the tools from the Post-Processing Toolkit, a variety of rich simulated scenarios can be created, such as rainy and night scenes. (f) RoCo-Sim can dynamically edit the foreground to generate simulated scenes with trajectory-based foreground objects, accurately maintaining front-to-back spatial relationships. As shown in the image, the simulated vehicle is occluded by the motorcycle when passing it, and it correctly generates vehicle shadows during movement.

data issues limit the performance of existing methods, causing poor performance on recently published datasets[8, 47].

Here, we highlight the key novelty of our approach. Unlike previous methods that focus on tweaking model architectures or laboriously annotating large datasets, we unleash the power of large-scale information-dense simulated data to dramatically enhance the performance of roadside perception models. Achieving this goal imposes several requirements on roadside simulation: simulations must be conducted using fixed-perspective inputs. The capability to edit scenes by inserting 3D foreground objects is essential for generating extensive simulated data. Then, the simulation must exhibit strong generalization capabilities, enabling deployment to new scenarios without extensive re-training, and produce photorealistic images.

However, many existing simulation methods are unsuitable for roadside perception tasks due to two key chal-

lenges: simulation with fixed-viewpoints and lack of 3D layouts for editing. As shown in Tab.1, methods based on NeRF [1, 27, 34, 37, 38, 43] and 3DGS [2, 34] cannot reconstruct under the conditions of roadside fixed sparse views, making them ineffective. Moreover, most methods[14, 26, 30, 32, 39, 45], that aim to generate simulated objects with 3D information rely on 3D layout inputs, which are lacking in roadside datasets. Traditional graphics engines like CARLA [4] manually simulate scenes without multi-view images but are time-consuming, labor-intensive, and lack realism, making them unsuitable for roadside scenarios. Furthermore, deploying roadside collaborative perception in real-world applications requires simulation methods that can generate large-scale data across diverse road scenarios without additional scene-specific training.

To address these challenges, we introduce RoCo-Sim, the first simulation framework designed for roadside col-

laborative perception. RoCo-Sim is capable of generating diverse, multi-view consistent simulated roadside data through dynamic foreground editing and full-scene style transfer of a single image, as shown in Fig. 2. Since the editing is performed in 3D space, our modifications made from one viewpoint can automatically propagate to other viewpoints, ensuring spatial consistency across multiple perspectives. The key design rationale behind RoCo-Sim is to leverage a rich 3D asset library to establish a 3D-to-2D mapping and, with the aid of graphical tools [3], seamlessly render foreground objects onto real 2D backgrounds. RoCo-Sim encompasses 4 key components: (i) Camera Extrinsic Optimization for accurate camera pose modeling; (ii) A novel Multi-View Occlusion-Aware Sampler (MOAS), which determines the occlusion-aware placement of digital assets within the 3D space, ensuring that assets are dynamically positioned in a physically plausible manner; (iii) DepthSAM, which innovatively models the foreground-background relationships in each viewpoint, enabling occlusion-aware insertion of 3D assets while maintaining multi-view consistency; and (iv) Scalable Post-Processing Toolkit for seamless integration through style transfer and other enhancements.

Extensive experiments are conducted on two real-world roadside datasets, RCooper [8] and TUMTraf-V2X [47], to evaluate RoCo-Sim. Our findings indicate that: i) Camera Extrinsic Optimization greatly improves model performance. Performance on RCooper improves by **62.55%** for AP70. ii) The performance improvement for perception becomes more significant as the amount of simulation data and the number of simulated vehicles per image increase. iii) RoCo-Sim significantly enhances perception performance. It enhances previous SOTA performance by **83.74%** on RCooper-Intersection and **83.12%** on TUMTraf-V2X for AP70. To sum up, our contributions are:

- We propose the first simulation framework for roadside collaborative perception, which simulates 3D foreground objects and renders them onto real 2D backgrounds.
- RoCo-Sim is a structured modular framework designed to generate diverse, multi-view consistent roadside simulation data through dynamic foreground editing and full-scene style transfer, while ensuring occlusion-aware asset placement and seamless integration for realistic and scalable simulation.
- We conduct extensive experiments on two real-world roadside datasets, validating that RoCo-Sim greatly enhances model performance, surpassing the impact of algorithmic improvements.

## 2. Related Work

**Camera-only 3D object detection.** Camera-based methods recover 3D information from 2D images and detect objects in a shared BEV feature space, either implicitly or

Table 1. Comparison of existing methods for autonomous driving simulation. “Fixed sparse views” refers to a setup where camera angles are fixed and limited in number. “Zero-shot” means the ability to perform without training on specific scenes.

Method	Photo-realistic	Dim.	Editable	Fixed sparse views	Zero-shot
CARLA [4]	×	3D	✓	✓	✓
BEVGen [26]	✓	2D	✓	×	×
BEVControl [39]	✓	2D	✓	×	×
DriveDreamer [30]	✓	2D	✓	×	×
DriveDreamer-2 [45]	✓	2D	✓	×	×
DrivingDiffusion [14]	✓	2D	✓	×	×
MagicDrive [5]	✓	2D	✓	×	×
MagicDrive3D [6]	✓	2D	✓	×	×
S-NeRF [38]	✓	3D	×	×	×
S-NeRF++ [1]	✓	3D	✓	×	×
UniSim [43]	✓	3D	✓	×	×
MARS [37]	✓	3D	✓	×	×
ChatSim [34]	✓	3D	✓	×	×
Omnire [2]	✓	3D	✓	×	×
<b>Roco-Sim(Ours)</b>	✓	3D-2D	✓	✓	✓

explicitly. Frustum-based methods [16, 22] predict depth distributions to form 3D frustums, then apply voxel pooling [15, 24] to extract BEV features. Query-based methods [17, 19, 31] use transformers to directly index 2D image features with 3D object queries. Recent approaches [28] incorporate streaming images to better utilize spatiotemporal information. While most methods focus on vision-centric BEV detection, roadside 3D object detection adapts frustum-based methods by estimating height [40] instead of depth. These methods focus on how to better extract spatiotemporal information from existing datasets.

**Collaborative perception.** Collaborative perception leverages multiple agents’ sensors to provide broader coverage with fewer blind spots [10]. Based on the stage of information transmission [21], it can be categorized into i) early fusion, which shares raw sensor data for complete perception but requires high bandwidth, ii) late fusion, which combines detected 3D boxes to save bandwidth but loses environmental details, and iii) intermediate fusion, which transmits low-resolution feature maps to balance performance and bandwidth [11, 33]. Existing systems mainly operate between vehicles or with a single roadside infrastructure [18, 42], while camera-only roadside collaborative perception remains unexplored due to data collection and calibration challenges. Our simulator addresses these challenges to advance this field.

**Realistic driving scenario simulation.** Current realistic scene simulation methods can be generally divided into two categories: image generation, and scene rendering. Some image generation works create realistic scene images that mimic data from real vehicle cameras. By employing advanced techniques like diffusion models [12, 14, 30, 32, 35], variational autoencoders [26], they can produce synthetic images tailored to various conditional requirements. However, most of them cannot maintain view consistency [5, 14, 26, 30, 35, 39] or can only generate data without producing corresponding bbox annotations [9, 13]. Another line of work based on NeRF [6, 20, 27, 34, 36, 38, 43]



or 3DGS [6, 46] targets to reconstruct the 3D scene and thus synthesize the camera visual image from novel views. However, this is not applicable in roadside scenarios, as the roadside cameras are fixed, making it difficult to achieve 3D modeling with multi-view cameras. Instead we focus on using 3D assets, and conduct multi-view camera and vehicle modeling, rendering the vehicle onto the background image to achieve foreground simulation, which ensures multi-view consistency while generating annotated simulation data.

### 3. Roadside Collaborative Simulation

As depicted in Fig.3, we introduce RoCo-Sim, the first simulation framework for roadside collaborative perception. It can generate diverse, multi-view consistent simulated roadside data from a single image and supports dynamic foreground editing and full-scene style transfer. Our key idea is to leverage a rich library of 3D assets to construct a 3D-to-2D mapping and render foreground objects onto real 2D backgrounds using graphical tools.

#### 3.1. Camera Extrinsic Optimizer

Optimization of camera extrinsics can effectively reduce the calibration error of fixed roadside cameras, thereby facilitating the accurate operation of the simulation. By mathematically modeling the 3D to 2D projection process and using optimization algorithms to reduce the errors in camera extrinsics, we develop a convenient calibration tool that is applicable to various roadside cameras.

To refine the extrinsic parameters of roadside cameras, we optimize the transformation matrix  $\mathcal{M}_{12c} = [\mathcal{R}|\mathcal{T}]$ , where  $\mathcal{R} \in SO(3)$  is the rotation matrix and  $\mathcal{T} \in \mathbb{R}^{3 \times 1}$  is the translation vector. Due to calibration errors, the actual transformation deviates from an ideal estimate  $\mathcal{M}_{12c}^*$ , leading to an extrinsic error  $\Delta\mathcal{M} = [\Delta\mathcal{R}|\Delta\mathcal{T}]$ , such that:

$$\mathcal{M}_{12c} = \mathcal{M}_{12c}^* + \Delta\mathcal{M} \quad (1)$$

This error affects the 2D projection, introducing a discrepancy between the projected bounding box points  $B_{2d} = \mathcal{K} \cdot [\mathcal{R}|\mathcal{T}] \cdot B_{3d}$  and the manually adjusted keypoints  $B'_{2d}$ , where  $B_{3d}$  represents the 3D coordinates of the bounding box corner points. We directly solving for  $\Delta\mathcal{M}$  by minimizing the projection error:

$$\min_{\Delta\mathcal{R}, \Delta\mathcal{T}} \|\mathcal{K} \cdot ([\mathcal{R}^* + \Delta\mathcal{R}|\mathcal{T}^* + \Delta\mathcal{T}]) \cdot B_{3d} - B'_{2d}\|^2 \quad (2)$$

subject to  $(\mathcal{R}^* + \Delta\mathcal{R})(\mathcal{R}^* + \Delta\mathcal{R})^T = \mathcal{I}$  to ensure  $\mathcal{R}$  remains a valid rotation, where  $\mathcal{K} \in \mathbb{R}^{3 \times 3}$  is the camera intrinsic matrix.  $\mathcal{I} \in \mathbb{R}^{3 \times 3}$  represents the identity matrix.  $\|\cdot\|^2$  represents L2 norm.

We employ the Broyden–Fletcher–Goldfarb–Shanno (BFGS) optimization algorithm, a quasi-Newton method

that iteratively approximates the inverse Hessian of the objective function to guide updates in  $\Delta\mathcal{R}$  and  $\Delta\mathcal{T}$ . Unlike first-order gradient descent methods, BFGS accelerates convergence by incorporating second-order curvature information, making it well-suited for non-linear optimization problems. We leverage solvers such as SciPy for efficient computation.

To further improve usability, we developed an interactive UI-based tool that allows users to manually adjust the projected bounding box, providing calibrated keypoints  $B'_{2d}$ , significantly reducing optimization complexity and improving efficiency. This tool will be released.

The optimized extrinsic matrix is then obtained as:

$$\mathcal{M}_{12c}^{opt} = [\mathcal{R}^{opt}|\mathcal{T}^{opt}] \quad (3)$$

ensuring precise projection alignment and correctly imaging 3D assets to reduce the distribution gap between simulated foregrounds and real foregrounds.

#### 3.2. Multi-View Occlusion-Aware Sampler

To address the sparsity of existing data and the limitation that current methods require a 3D layout for editing, we introduce the Multi-View Occlusion-Aware Sampler (MOAS). MOAS automatically determines the placement of digital assets within a 3D space based on the distribution of objects in the scene. The placements must meet two criteria: they should be widely dispersed, and visible from multiple viewpoints while ensuring physical plausibility (e.g., no collisions). To achieve this, we sample potential placement points from locations where real objects have appeared and use a scorer to select sampling regions and a checker to detect insertability.

**Optimization-based scorer.** We divide the entire 3D space into multiple grids, score these grids to determine the selected placement areas, and randomly sample within them. The score is determined by the sum of two optimization objectives, where a higher score indicates better placement strategy.

One optimization objective is to maximize the visibility of placement positions from multiple perspectives while ensuring that these perspectives are as evenly distributed as possible; that is:

$$\text{avg} = \frac{\sum_{m \in M} (V_m(p_i))}{|M|} \quad (4)$$

$$V_i = \sum_{m \in M} V_m(p_i) - \sum_{m \in M} (V_m(p_i) - \text{avg})^2 \quad (5)$$

where  $M$  is the camera lists,  $|\cdot|$  is the cardinal of set.  $p_i$  represents the chosen insert points.  $V_m(p_i)$  indicates whether  $p_i$  is visible in camera  $m$ ; if it is visible, the value is 1; otherwise, it is 0.  $V_i$  measures the visibility and coverage of the field of view for the  $i$ -th placed point.



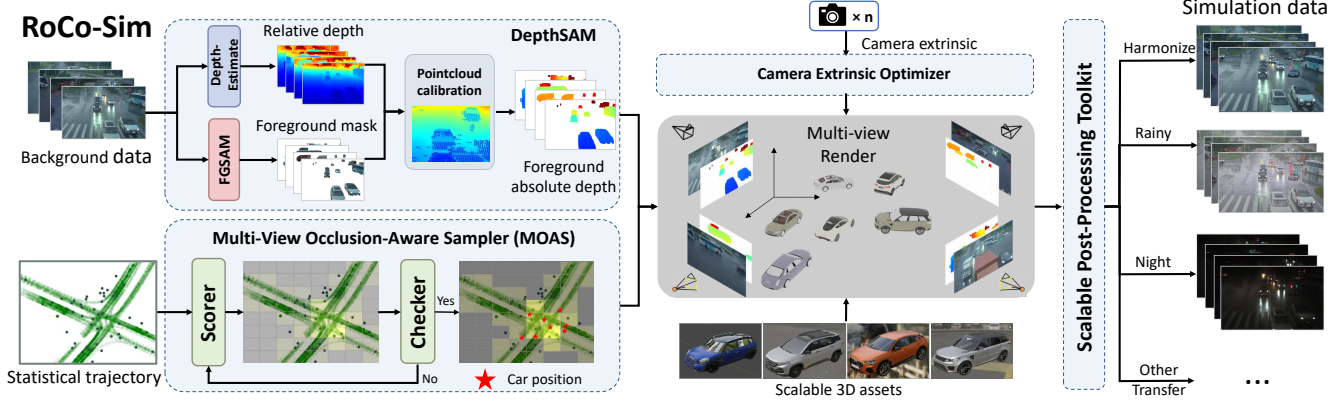


Figure 3. **Overview of RoCo-Sim.** RoCo-Sim consists of four components: (1) Camera Extrinsic Optimization ensures accurate roadside cameras modeling; (2) Multi-View Occlusion-Aware Sampler (MOAS) determines the placement of diverse digital assets within 3D space; (3) DepthSAM ensures that rendering adheres to front-to-back relationships and correct occlusion between objects; and (4) Scalable Post-Processing Toolkit is an expandable toolkit capable of generating more diverse and enriched scenes.

Another optimization objective is to maximize the distance between points, ensuring that the distribution of placed vehicles is as dispersed as possible, which creates a richer set of placement points. That is:

$$O = \frac{\sum_{p_i \in P} \sum_{p_j \in P} \|p_i - p_j\|^2}{2 \cdot |P|} \quad (6)$$

where  $P$  represents the set of current selection of placement points and existing vehicles.  $O$  is used to measure the average distances between all points. To achieve multi-view visibility with as uniform distribution as possible, we define the ultimate optimization goal as :

$$\max_P \left[ \sum_{p_i \in P} V_i + \frac{\sum_{p_i \in P} \sum_{p_j \in P} \|p_i - p_j\|^2}{2 \cdot |P|} \right]$$

**Rule-based checker.** After determining the sampling points, we need to check whether these points are placeable under the distribution conditions. The placement of new objects must satisfy two main conditions: 1) In 3D space, there should be no overlapping with existing simulated objects or real objects; 2) The object should be visible from at least one camera perspective when projected across multiple camera views. The first condition ensures that the simulated scene complies with physical laws, such as preventing objects from collisions. The second condition ensures that the inserted object is visible in the rendered image. Each insertion requires checking these two conditions to determine the final feasible placement location, enabling adaptive object placement.

### 3.3. DepthSAM

After modeling the camera and 3D foreground objects, we render them onto a 2D image while maintaining their 3D spatial relationships. To achieve this, we require a

highly generalizable depth estimation method. However, existing approaches often struggle with ground and sky regions and lack absolute depth information. We address this by segmenting foreground objects, extracting their depth, and calibrating it with point cloud data to obtain accurate foreground depth for rendering while preserving multi-view consistency.

Given an image  $I \in \mathbb{R}^{H \times W \times 3}$ , we can perform segmentation [44] to obtain the segmentation set  $S(I) = \{S_0, S_1, \dots, S_m\}$ ,  $m$  represents the number of instances segmented in the image. Using the annotation information, we can determine the center points of each foreground object  $C_{\text{bbox}} = \{c_0, c_1, \dots, c_n\}$ , thus obtaining the foreground segmentation as follows:

$$S_{\text{foreground}} = \left\{ S_i \mid S_i \subseteq S(I), N(S_i) < \frac{H \cdot W}{4} \right. \\ \left. \text{and } \exists c_j \in C_{\text{bbox}}, \text{ s.t. } c_j \in S_i \right\} \quad (7)$$

The number of points in  $S_i$ , denoted as  $N(S_i)$ , should satisfy the condition  $N(s_i) < \frac{H \cdot W}{4}$  to filter the ground and sky. According to our statistics, the size of foreground objects typically does not exceed  $\frac{H \cdot W}{4}$ . Then we can get mask  $M \in \mathbb{R}^{H \times W}$  as follows:

$$M(u, v) = \begin{cases} 1, & \text{if } (u, v) \in S_{\text{foreground}} \\ 0, & \text{otherwise} \end{cases} \quad (8)$$

We denotes  $D_{\text{rel}} \in \mathbb{R}^{H \times W}$  represents the relative depth predicted by DepthAnything [41] and  $Z \in \mathbb{R}^{H \times W}$  represents the projected depth map. The projected depth is obtained from a 3D point cloud  $P_{3d} \in \mathbb{R}^{N \times 3}$ , where  $N$  is the number of points. The point cloud is projected into the camera coordinate system using  $P_{\text{cam}} = M_{12c} \cdot P_{3d}$ . The depth value  $Z(u, v)$  satisfying  $Z(u, v) \cdot (u, v, 1)^T = \mathcal{K} \cdot P_{\text{cam}}$  for pixel  $(u, v)$ . We solve for the calibration parameters  $a$  and  $b$  using the following optimization problem:

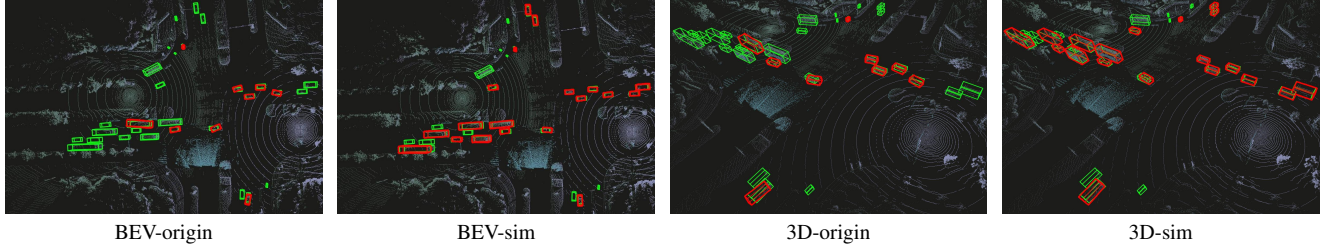


Figure 4. The model trained with simulated data boosts vehicle detection. Green and red boxes denote GT and detection respectively.

$$\min_{a,b} \sum_{(u,v) \in P_{2d}} \|a \cdot D_{rel}(u,v) + b - Z(u,v)\|^2 \quad (9)$$

where  $P_{2d}$  is the set of 2D pixels in the image,  $a$  and  $b$  are the scaling factor and offset, respectively. They transform the relative depth  $D_{rel}$  into absolute depth via  $a \cdot D_{rel}(u,v) + b$ . The calibrated foreground depth  $D_{final}$  is defined as:

$$D_{final} = \begin{cases} a \cdot D_{rel}(u,v) + b, & M(u,v) = 1 \\ +\infty, & M(u,v) = 0 \end{cases} \quad (10)$$

DepthSAM extracts pixel-level depth for foreground objects, ensuring correct occlusion and depth order during 3D-to-2D rendering, which guarantees multi-view consistency.

### 3.4. Scalable Post-Processing Toolkit

To elevate the diversity of simulation scenarios and embrace a future-oriented approach, we design a scalable post-processing toolkit for RoCo-Sim. This toolkit provides a modular interface that seamlessly integrates a wide array of innovative image processing tools, including style transfer, scene transformation, and more. By doing so, it not only significantly enhances the diversity of the generated data but also paves the way for continuous expansion, allowing the incorporation of more sophisticated post-processing techniques to enrich the simulation environment.

## 4. Experiment

In this section, we introduce our experimental setting and evaluate the effectiveness of RoCo-Sim on two roadside camera-only detection models. All experiments are conducted using the optimized extrinsic parameters obtained from Eq. 3 by default. Results show RoCo-Sim boosts performance in both cases, which proves RoCo-Sim’s value. We report the average precision at 40 recall points ( $AP_{3D|R40}$ ) [7] for 3D bounding boxes and assess the improvements in network capability driven by simulated data using the KITTI evaluation metrics.

### 4.1. Datasets

We use two of the latest road-side collaborative perception datasets: Rcooper-Intersection [8] and TUMTraf-

V2X [47]. We conduct simulations across three traffic scenarios in both datasets to evaluate the impact of simulation on improving the performance of 3D object detection tasks.

**Rcooper-Intersection.** We focus specifically on intersection scenarios due to their higher visual information overlap, which facilitates collaborative perception. The Rcooper-Intersection dataset comprises two traffic scenarios: 117-118-120-119 and 136-137-138-139 (hereafter referred to as 117 and 136, respectively).

**TUMTraf-V2X.** To assess the generalization improvements from simulation, we avoid the official data splits, where target information in training and validation sets is nearly identical. Instead, we apply temporal partitioning, sorting data chronologically into sequences of 40 images and using the last two sequences (13th and 14th) for validation. This ensures a temporal separation between training and validation sets, preventing misleading performance gains from overfitting.

### 4.2. Implementation Details

**Perception model.** We conduct experiments using BEVHeight [40] and BEVSpread [29], setting the perception range to 0–150 meters with ResNet-101 as the image backbone. The grid size is fixed at 0.4 meters, and the initial learning rate is set to  $2e-4$ . All experiments are conducted on two RTX-4090 GPUs, with models trained for 40 epochs, ensuring proper convergence.

**Simulation baseline.** Currently, no simulation methods are designed for roadside scenarios. Existing vehicle-side approaches rely on multi-view cameras or 3D reconstruction techniques like NeRF and 3DGS, which are unsuitable for fixed roadside cameras. Additionally, many simulation methods that generate 3D bounding boxes for downstream tasks require 3D layout inputs, which roadside datasets lack, limiting their applicability.

### 4.3. Simulation Results

From Fig.2, it can be seen that RoCo-Sim demonstrates outstanding simulation performance, addressing various data issues and overcoming the challenges of roadside simulation. Fig.2 (a) highlights the critical impact of extrinsic parameter optimization on data annotation, effectively correcting a significant number of projection errors

Table 2. RoCo-Sim greatly enhances detection performance, even surpassing those achieved by the optimized model BEVSpread.

Backbone	Roco-Sim	Rcooper-117					Rcooper-136				
		origin/aug	bev@0.5	3D@0.5	bev@0.7	3D@0.7	origin/aug	bev@0.5	3D@0.5	bev@0.7	3D@0.7
BEVHeight	×	5120/0	65.3233	56.1948	46.9456	31.8694	1632/0	22.6618	14.8236	13.6882	7.2549
	✓	5120/2400	<b>77.6463</b>	<b>71.5983</b>	<u>50.6319</u>	<b>42.0199</b>	1632/4500	<b>40.3816</b>	<u>33.1069</u>	<b>29.9080</b>	<u>16.6990</u>
BEVSpread	×	5120/0	66.3986	57.4217	48.2224	34.5299	1632/0	36.5752	30.0382	21.5373	13.2292
	✓	5120/2400	<u>75.5791</u>	<u>69.3342</u>	<b>56.1572</b>	<u>40.6480</u>	1632/4500	<u>40.1567</u>	<b>36.0443</b>	<u>29.6339</u>	<b>19.0902</b>

Backbone	Roco-Sim	Rcooper-117+Rcooper-136					TUM				
		origin/aug	bev@0.5	3D@0.5	bev@0.7	3D@0.7	origin/aug	bev@0.5	3D@0.5	bev@0.7	3D@0.7
BEVHeight	×	6752/0	36.1190	21.5442	19.9593	10.8835	2400/0	54.8044	45.4383	28.3148	13.1911
	✓	6752/9000	<u>54.6708</u>	37.4621	<u>36.6740</u>	15.0132	2400/2400	<u>57.0037</u>	43.8220	<u>35.4583</u>	<b>24.1557</b>
BEVSpread	×	6752/0	53.5341	<u>43.8613</u>	34.7345	<u>20.1353</u>	2400/0	52.8383	43.3036	32.2100	19.8507
	✓	6752/9000	<b>54.9626</b>	<b>48.9011</b>	<b>38.8669</b>	<b>26.7668</b>	2400/2400	<b>59.3968</b>	<b>48.5001</b>	<b>37.0695</b>	<u>23.0567</u>

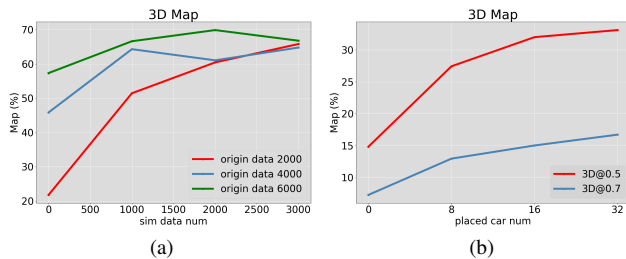


Figure 5. (a) More simulations improve performance, allowing small-scale original data to achieve results comparable to larger datasets. (b) As the number of simulated vehicles increases, model performance improves.

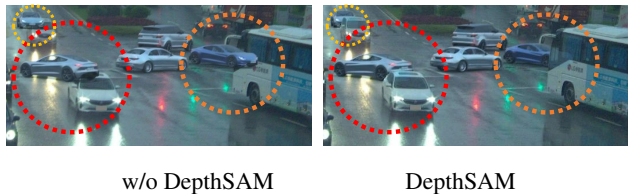


Figure 6. Without DepthSAM, simulated vehicles may overlap with existing ones, disrupting spatial relationships.

in the annotations. Fig.2 (b) illustrates that simulated vehicles seem to float before optimization due to inaccurate extrinsic parameters affecting camera modeling. After optimization, vehicles are more realistically aligned with the ground, as correct extrinsic parameters ensure precise rendering of simulated objects. Fig.2 (c) shows that RoCo-Sim correctly determines the relative depth order between simulated and real vehicles, further validating the effectiveness of DepthSAM. Fig. 2 (d) illustrates RoCo-Sim’s multi-view consistency for simulated vehicles. With MOAS and DepthSAM, vehicle placement is sensible, projections are accurate, and there are correct occlusion relationships between objects across views. Fig.2 (e) shows very realistic simulations with four vehicles added to a real scene, making the synthetic parts hard to spot. It also showcases RoCo-Sim’s potential to generate diverse data, such as in rainy and night conditions, using the Scalable Post-Processing Toolkit. Fig. 2 (f) illustrates the dynamic foreground editing.

#### 4.4. Perception Evaluation

**RoCo-Sim significantly enhances both roadside perception and late fusion in roadside cooperative perception.** Performance results are shown in Fig.1, for BEVHeight, we see major improvements: AP3D 50 rises by 27.4%, 143.2%, 127.0% for Rcooper in scenarios 117, 136, and 117-136. More numerical results are shown in Tab. 2, demonstrating simulation data’s strong impact. Tab. 3 underscores late fusion’s role in enhancing perception by combining multi-view data beyond single-camera capabilities. In Tab. 2, labels are limited to 3D annotations visible in the image, while Tab. 3 includes all 3D scene objects, even those outside the camera view. Fig. 4 shows that models trained with additional simulation data can detect more objects in the late fusion stage. Moreover, the positions and orientations of the bounding boxes are more accurate.

**The performance improvement through RoCo-Sim far exceeds that of algorithm enhancements.** Comparing with the newer BEVSpread [29], we find that BEVHeight [40] trained on simulation data outperforms BEVSpread trained on original data. This finding highlights that simulated data not only enhances performance but can surpass gains from algorithmic improvements.

**Impact of simulation data scale and vehicles.** We study how adding simulated data to different initial data sizes on the 117 dataset affects results, as shown in Fig. 5 (a). Mixing just 2000 original images with lots of simulated data greatly improves network performance, matching that of networks trained on large real datasets. This shows simulated data can effectively supplement real data. We also look at detection performance changes on the 136 dataset as the number of simulated vehicles increased, as in Fig. 5 (b). More vehicles mean better detection, suggesting we can use fewer simulations by adding more vehicles to get similar results, cutting training costs.

#### 4.5. Ablation studies

We validate key components of RoCo-Sim. The scalable post-processing toolkit enhances style diversity for bet-



Table 3. Incorporating simulated data generated by RoCo-sim improves late fusion performance in both models.

Backbone	Roco-Sim	Rcooper-117					Rcooper-136				
		origin/aug	bev@0.5	3D@0.5	bev@0.7	3D@0.7	origin/aug	bev@0.5	3D@0.5	bev@0.7	3D@0.7
BEVHeight	×	5120/0	12.8650	7.3672	7.1578	3.7598	1632/0	14.3390	9.0959	8.1261	4.0682
	✓	5120/2400	<u>16.6556</u>	<u>16.2424</u>	<u>13.0317</u>	<u>9.3716</u>	1632/4500	15.2574	9.0587	<b>21.1498</b>	<b>17.6615</b>
BEVSpread	×	5120/0	16.5150	13.6578	10.7850	7.7328	1632/0	<u>20.5816</u>	<u>17.0001</u>	13.2643	7.7018
	✓	5120/2400	<b>16.9561</b>	<b>16.3672</b>	<b>13.1573</b>	<b>10.0375</b>	1632/2400	<b>21.3933</b>	<b>18.3458</b>	<u>15.0851</u>	<u>11.0922</u>

Backbone	Roco-Sim	Rcooper-117+Rcooper-136					TUM				
		origin/aug	bev@0.5	3D@0.5	bev@0.7	3D@0.7	origin/aug	bev@0.5	3D@0.5	bev@0.7	3D@0.7
BEVHeight	×	6752/0	14.7159	8.7044	8.3179	4.0130	2400/0	<u>42.7962</u>	<b>33.1987</b>	18.6450	8.9220
	✓	6752/9000	<b>21.4400</b>	<b>17.8329</b>	<u>14.7487</u>	<u>7.6758</u>	2400/2400	42.4077	<u>33.1671</u>	<b>25.1554</b>	<b>16.0500</b>
BEVSpread	×	6752/0	13.5685	12.3687	9.7065	6.8483	2400/0	40.7025	31.6073	21.4561	<u>14.0298</u>
	✓	6752/9000	<u>19.0796</u>	<u>16.3904</u>	<b>14.8512</b>	<b>9.3302</b>	2400/2400	<b>44.9000</b>	32.1661	<u>22.8040</u>	13.2693

Table 4. Camera Extrinsic Optimization improves detection performance

Dataset	Calib	bev@0.5	3D@0.5	bev@0.7	3D@0.7
117	×	39.6378	33.0679	25.3091	19.6054
	✓	<u>65.3233</u>	56.1948	46.9456	31.8694
136	×	18.2512	12.8897	10.8723	7.9102
	✓	<u>22.6618</u>	14.8236	13.6882	7.2549
117-136	×	32.2033	19.6822	17.9436	6.2302
	✓	<u>36.1190</u>	21.5442	19.9593	10.8835

Table 5. Scorer increases the number and diversity of vehicles rendered onto images, Checker prevents object overlap, and DepthSAM ensures correct depth relationships during rendering. All contribute to better simulation data generation and improved model detection performance.

DepthSAM	Scorer	Checker	bev@0.5	3D@0.5	bev@0.7	3D@0.7
✓			31.2110	19.6172	18.7138	9.6544
✓		✓	38.2746	23.3362	23.0323	9.0517
✓	✓		33.1691	21.4200	22.9378	9.4178
	✓	✓	37.2985	16.9951	21.5125	5.5527
✓	✓	✓	<b>39.5758</b>	<b>31.9978</b>	<b>25.7230</b>	<b>15.0032</b>

ter generalization and real-world deployment, but in the ablation study, it is only used to maintain foreground-background style consistency.

**Camera extrinsic optimization algorithm.** From Tab. 4, we find that calibrating the camera extrinsics can significantly enhance model performance. For instance, in the case of 117, as shown in Fig. 2, the extrinsics are quite inaccurate, resulting in a 62.55% improvement in performance for AP70 after calibration. This is because camera extrinsics calibration aligns the images and labels, making it easier for the model to learn useful information from them.

**DepthSAM.** From Tab. 5, We find that without DepthSAM, performance is poor and may even decline in AP70. This is because, without DepthSAM, vehicles behind in the original image can obscure those in front during rendering, as show in Fig. 6, leading to a violation of the spatial relationships and resulting in decreased performance.

**MOAS.** From Tab. 5, we find that both the Scorer and

Checker contribute to enhancing the quality of generated simulation data. The Scorer macroscopically regulates vehicle placement to allow for more visibility with the same number of vehicles, thus increasing the data scale. Meanwhile, the Checker ensures that the inserted vehicles do not conflict in 3D space and are visible in the projected image. We can also see that the impact of checker is greater than that of scorer. This is because without checker, the placed simulated vehicles would overlap, which is not possible in the real world, making it difficult for the model to learn.

## 5. Conclusion

This work unleashes the power of simulation data to enhance roadside collaborative perception, demonstrating that simulation data, rather than model architecture, is the **true winner** in performance competition. The proposed RoCo-Sim is the first simulation framework specifically designed for roadside collaborative perception. RoCo-Sim generates a large scale of multi-view consistent simulation data from sparse fixed viewpoints, supports both foreground editing and full-scene style transformation, and can be rapidly deployed to any new road environment. We hope this work will significantly accelerate the practical development of roadside collaborative perception, ultimately enhancing driving safety.

**Limitation and future work.** Current 3D assets are limited in variety, and manually constructing them is costly. Therefore, it is important to explore new methods for generating diverse 3D assets. Besides, a trajectory generator that considers real-world traffic flow and regulations could further enhance the realism of virtual vehicle distributions. Additionally, we find that existing models experience a significant performance drop when applied to a new intersection. In the future, we hope that our simulation framework can help train detection models with stronger generalization capabilities.

## References

- [1] Yurui Chen, Junge Zhang, Ziyang Xie, Wenye Li, Feihu Zhang, Jiachen Lu, and Li Zhang. S-nerf++: Autonomous driving simulation via neural reconstruction and generation. *arXiv preprint arXiv:2402.02112*, 2024. 2, 3
- [2] Ziyu Chen, Jiawei Yang, Jiahui Huang, Riccardo de Lutio, Janick Martinez Esturo, Boris Ivanovic, Or Litany, Zan Gojcic, Sanja Fidler, Marco Pavone, et al. Omnire: Omni urban scene reconstruction. *arXiv preprint arXiv:2408.16760*, 2024. 2, 3
- [3] Blender Online Community. *Blender - a 3D modelling and rendering package*. Blender Foundation, Stichting Blender Foundation, Amsterdam, 2018. 3
- [4] Alexey Dosovitskiy, German Ros, Felipe Codevilla, Antonio Lopez, and Vladlen Koltun. Carla: An open urban driving simulator. In *Conference on robot learning*, pages 1–16. PMLR, 2017. 2, 3
- [5] Ruiyuan Gao, Kai Chen, Enze Xie, Lanqing Hong, Zhenguao Li, Dit-Yan Yeung, and Qiang Xu. Magicdrive: Street view generation with diverse 3d geometry control. *arXiv preprint arXiv:2310.02601*, 2023. 3
- [6] Ruiyuan Gao, Kai Chen, Zhihao Li, Lanqing Hong, Zhenguao Li, and Qiang Xu. Magicdrive3d: Controllable 3d generation for any-view rendering in street scenes. *arXiv preprint arXiv:2405.14475*, 2024. 3, 4
- [7] Andreas Geiger, Philip Lenz, and Raquel Urtasun. Are we ready for autonomous driving? the kitti vision benchmark suite. In *2012 IEEE conference on computer vision and pattern recognition*, pages 3354–3361. IEEE, 2012. 6
- [8] Ruiyang Hao, Siqi Fan, Yingru Dai, Zhenlin Zhang, Chenxi Li, Yuntian Wang, Haibao Yu, Wenxian Yang, Jirui Yuan, and Zaiqing Nie. Rcooper: A real-world large-scale dataset for roadside cooperative perception. In *Proceedings of the IEEE/CVF Conference on Computer Vision and Pattern Recognition*, pages 22347–22357, 2024. 1, 2, 3, 6
- [9] Anthony Hu, Lloyd Russell, Hudson Yeo, Zak Murez, George Fedoseev, Alex Kendall, Jamie Shotton, and Gianluca Corrado. Gaia-1: A generative world model for autonomous driving. *arXiv preprint arXiv:2309.17080*, 2023. 3
- [10] Yue Hu, Shaoheng Fang, Zixing Lei, Yiqi Zhong, and Siheng Chen. Where2comm: Communication-efficient collaborative perception via spatial confidence maps. *Advances in neural information processing systems*, 35:4874–4886, 2022. 3
- [11] Yue Hu, Yifan Lu, Runsheng Xu, Weidi Xie, Siheng Chen, and Yanfeng Wang. Collaboration helps camera overtake lidar in 3d detection. in 2023 ieee. In *CVF Conference on Computer Vision and Pattern Recognition (CVPR)*, page 5, 2023. 3
- [12] Binyuan Huang, Yuqing Wen, Yucheng Zhao, Yaosi Hu, Yingfei Liu, Fan Jia, Weixin Mao, Tiancai Wang, Chi Zhang, Chang Wen Chen, et al. Subjectdrive: Scaling generative data in autonomous driving via subject control. *arXiv preprint arXiv:2403.19438*, 2024. 3
- [13] Fan Jia, Weixin Mao, Yingfei Liu, Yucheng Zhao, Yuqing Wen, Chi Zhang, Xiangyu Zhang, and Tiancai Wang. Adriver-i: A general world model for autonomous driving. *arXiv preprint arXiv:2311.13549*, 2023. 3
- [14] Xiaofan Li, Yifu Zhang, and Xiaoqing Ye. Drivingdiffusion: Layout-guided multi-view driving scene video generation with latent diffusion model. *arXiv preprint arXiv:2310.07771*, 2023. 2, 3
- [15] Yinhao Li, Han Bao, Zheng Ge, Jinrong Yang, Jianjian Sun, and Zeming Li. Bevstereo: Enhancing depth estimation in multi-view 3d object detection with temporal stereo. In *Proceedings of the AAAI Conference on Artificial Intelligence*, pages 1486–1494, 2023. 3
- [16] Yinhao Li, Zheng Ge, Guanyi Yu, Jinrong Yang, Zengran Wang, Yukang Shi, Jianjian Sun, and Zeming Li. Bevdepth: Acquisition of reliable depth for multi-view 3d object detection. In *Proceedings of the AAAI Conference on Artificial Intelligence*, pages 1477–1485, 2023. 1, 3
- [17] Zhiqi Li, Wenhai Wang, Hongyang Li, Enze Xie, Chonghao Sima, Tong Lu, Yu Qiao, and Jifeng Dai. Bevformer: Learning bird’s-eye-view representation from multi-camera images via spatiotemporal transformers. In *European conference on computer vision*, pages 1–18. Springer, 2022. 3
- [18] Genjia Liu, Yue Hu, Chenxin Xu, Weibo Mao, Junhao Ge, Zhengxiang Huang, Yifan Lu, Yinda Xu, Junkai Xia, Yafei Wang, et al. Towards collaborative autonomous driving: Simulation platform and end-to-end system. *arXiv preprint arXiv:2404.09496*, 2024. 3
- [19] Yingfei Liu, Junjie Yan, Fan Jia, Shuailin Li, Aqi Gao, Tiancai Wang, and Xiangyu Zhang. Petrv2: A unified framework for 3d perception from multi-camera images. In *Proceedings of the IEEE/CVF International Conference on Computer Vision*, pages 3262–3272, 2023. 3
- [20] William Ljungbergh, Adam Tonderski, Joakim Johlander, Holger Caesar, Kalle Åström, Michael Felsberg, and Christoffer Petersson. Neuroncap: Photorealistic closed-loop safety testing for autonomous driving. In *European Conference on Computer Vision*, pages 161–177. Springer, 2025. 3
- [21] Yifan Lu, Yue Hu, Yiqi Zhong, Dequan Wang, Yanfeng Wang, and Siheng Chen. An extensible framework for open heterogeneous collaborative perception. *arXiv preprint arXiv:2401.13964*, 2024. 3
- [22] Jonah Philion and Sanja Fidler. Lift, splat, shoot: Encoding images from arbitrary camera rigs by implicitly unprojecting to 3d. In *Computer Vision—ECCV 2020: 16th European Conference, Glasgow, UK, August 23–28, 2020, Proceedings, Part XIV 16*, pages 194–210. Springer, 2020. 3
- [23] Zequn Qin and Xi Li. Monoground: Detecting monocular 3d objects from the ground. In *Proceedings of the IEEE/CVF Conference on Computer Vision and Pattern Recognition*, pages 3793–3802, 2022. 1
- [24] Cody Reading, Ali Harakeh, Julia Chae, and Steven L Waslander. Categorical depth distribution network for monocular 3d object detection. In *Proceedings of the IEEE/CVF Conference on Computer Vision and Pattern Recognition*, pages 8555–8564, 2021. 3
- [25] Ziyang Song, Lin Liu, Feiyang Jia, Yadan Luo, Caiyan Jia, Guoxin Zhang, Lei Yang, and Li Wang. Robustness-aware

- 3d object detection in autonomous driving: A review and outlook. *IEEE Transactions on Intelligent Transportation Systems*, 2024. 1
- [26] Alexander Swerdlow, Runsheng Xu, and Bolei Zhou. Street-view image generation from a bird’s-eye view layout. *IEEE Robotics and Automation Letters*, 2024. 2, 3
- [27] Adam Tonderski, Carl Lindström, Georg Hess, William Ljungbergh, Lennart Svensson, and Christoffer Petersson. Neurad: Neural rendering for autonomous driving. In *Proceedings of the IEEE/CVF Conference on Computer Vision and Pattern Recognition*, pages 14895–14904, 2024. 2, 3
- [28] Shihao Wang, Yingfei Liu, Tiancai Wang, Ying Li, and Xiangyu Zhang. Exploring object-centric temporal modeling for efficient multi-view 3d object detection. In *Proceedings of the IEEE/CVF International Conference on Computer Vision*, pages 3621–3631, 2023. 3
- [29] Wenjie Wang, Yehao Lu, Guangcong Zheng, Shuigen Zhan, Xiaoqing Ye, Zichang Tan, Jingdong Wang, Gaoang Wang, and Xi Li. Bevsprad: Spread voxel pooling for bird’s-eye-view representation in vision-based roadside 3d object detection. In *Proceedings of the IEEE/CVF Conference on Computer Vision and Pattern Recognition*, pages 14718–14727, 2024. 1, 6, 7
- [30] Xiaofeng Wang, Zheng Zhu, Guan Huang, Xinze Chen, Jiagang Zhu, and Jiwen Lu. Drivedreamer: Towards real-world-driven world models for autonomous driving. *arXiv preprint arXiv:2309.09777*, 2023. 2, 3
- [31] Yue Wang, Vitor Campagnolo Guizilini, Tianyuan Zhang, Yilun Wang, Hang Zhao, and Justin Solomon. Detr3d: 3d object detection from multi-view images via 3d-to-2d queries. In *Conference on Robot Learning*, pages 180–191. PMLR, 2022. 3
- [32] Yuqi Wang, Jiawei He, Lue Fan, Hongxin Li, Yuntao Chen, and Zhaoxiang Zhang. Driving into the future: Multiview visual forecasting and planning with world model for autonomous driving. In *Proceedings of the IEEE/CVF Conference on Computer Vision and Pattern Recognition*, pages 14749–14759, 2024. 2, 3
- [33] Sizhe Wei, Yuxi Wei, Yue Hu, Yifan Lu, Yiqi Zhong, Siheng Chen, and Ya Zhang. Asynchrony-robust collaborative perception via bird’s eye view flow. *Advances in Neural Information Processing Systems*, 36, 2024. 3
- [34] Yuxi Wei, Zi Wang, Yifan Lu, Chenxin Xu, Changxing Liu, Hao Zhao, Siheng Chen, and Yanfeng Wang. Editable scene simulation for autonomous driving via collaborative llm-agents. In *Proceedings of the IEEE/CVF Conference on Computer Vision and Pattern Recognition*, pages 15077–15087, 2024. 2, 3
- [35] Yuqing Wen, Yucheng Zhao, Yingfei Liu, Fan Jia, Yanhui Wang, Chong Luo, Chi Zhang, Tiancai Wang, Xiaoyan Sun, and Xiangyu Zhang. Panacea: Panoramic and controllable video generation for autonomous driving. In *Proceedings of the IEEE/CVF Conference on Computer Vision and Pattern Recognition*, pages 6902–6912, 2024. 3
- [36] Chenming Wu, Jiadai Sun, Zhelun Shen, and Liangjun Zhang. Mapnerf: Incorporating map priors into neural radiance fields for driving view simulation. In *2023 IEEE/RSJ International Conference on Intelligent Robots and Systems (IROS)*, pages 7082–7088. IEEE, 2023. 3
- [37] Zirui Wu, Tianyu Liu, Liyi Luo, Zhide Zhong, Jianteng Chen, Hongmin Xiao, Chao Hou, Haozhe Lou, Yuantao Chen, Runyi Yang, et al. Mars: An instance-aware, modular and realistic simulator for autonomous driving. In *CAAI International Conference on Artificial Intelligence*, pages 3–15. Springer, 2023. 2, 3
- [38] Ziyang Xie, Junge Zhang, Wenye Li, Feihu Zhang, and Li Zhang. S-nerf: Neural radiance fields for street views. *arXiv preprint arXiv:2303.00749*, 2023. 2, 3
- [39] Kairui Yang, Enhui Ma, Jibin Peng, Qing Guo, Di Lin, and Kaicheng Yu. Bevcontrol: Accurately controlling street-view elements with multi-perspective consistency via bev sketch layout. *arXiv preprint arXiv:2308.01661*, 2023. 2, 3
- [40] Lei Yang, Kaicheng Yu, Tao Tang, Jun Li, Kun Yuan, Li Wang, Xinyu Zhang, and Peng Chen. Bevheight: A robust framework for vision-based roadside 3d object detection. In *Proceedings of the IEEE/CVF Conference on Computer Vision and Pattern Recognition*, pages 21611–21620, 2023. 1, 3, 6, 7
- [41] Lihe Yang, Bingyi Kang, Zilong Huang, Zhen Zhao, Xiaogang Xu, Jiashi Feng, and Hengshuang Zhao. Depth anything v2. *arXiv preprint arXiv:2406.09414*, 2024. 5
- [42] Lei Yang, Xinyu Zhang, Jiaxin Yu, Jun Li, Tong Zhao, Li Wang, Yi Huang, Chuang Zhang, Hong Wang, and Yiming Li. Monogae: Roadside monocular 3d object detection with ground-aware embeddings. *IEEE Transactions on Intelligent Transportation Systems*, 2024. 3
- [43] Ze Yang, Yun Chen, Jingkang Wang, Sivabalan Manivasagam, Wei-Chiu Ma, Anqi Joyce Yang, and Raquel Urtasun. Unisim: A neural closed-loop sensor simulator. In *Proceedings of the IEEE/CVF Conference on Computer Vision and Pattern Recognition*, pages 1389–1399, 2023. 2, 3
- [44] Chaoning Zhang, Dongshen Han, Yu Qiao, Jung Uk Kim, Sung-Ho Bae, Seungkyu Lee, and Choong Seon Hong. Faster segment anything: Towards lightweight sam for mobile applications. *arXiv preprint arXiv:2306.14289*, 2023. 5
- [45] Guosheng Zhao, Xiaofeng Wang, Zheng Zhu, Xinze Chen, Guan Huang, Xiaoyi Bao, and Xingang Wang. Drivedreamer-2: Llm-enhanced world models for diverse driving video generation. *arXiv preprint arXiv:2403.06845*, 2024. 2, 3
- [46] Xiaoyu Zhou, Zhiwei Lin, Xiaojun Shan, Yongtao Wang, Deqing Sun, and Ming-Hsuan Yang. Drivinggaussian: Composite gaussian splatting for surrounding dynamic autonomous driving scenes. In *Proceedings of the IEEE/CVF Conference on Computer Vision and Pattern Recognition*, pages 21634–21643, 2024. 4
- [47] Walter Zimmer, Gerhard Arya Wardana, Suren Sritharan, Xingcheng Zhou, Rui Song, and Alois C Knoll. Tumor-traffic v2x cooperative perception dataset. In *Proceedings of the IEEE/CVF Conference on Computer Vision and Pattern Recognition*, pages 22668–22677, 2024. 2, 3, 6





Figure 1. Camera Extrinsic Optimization results of 16 cameras of Rcooper.

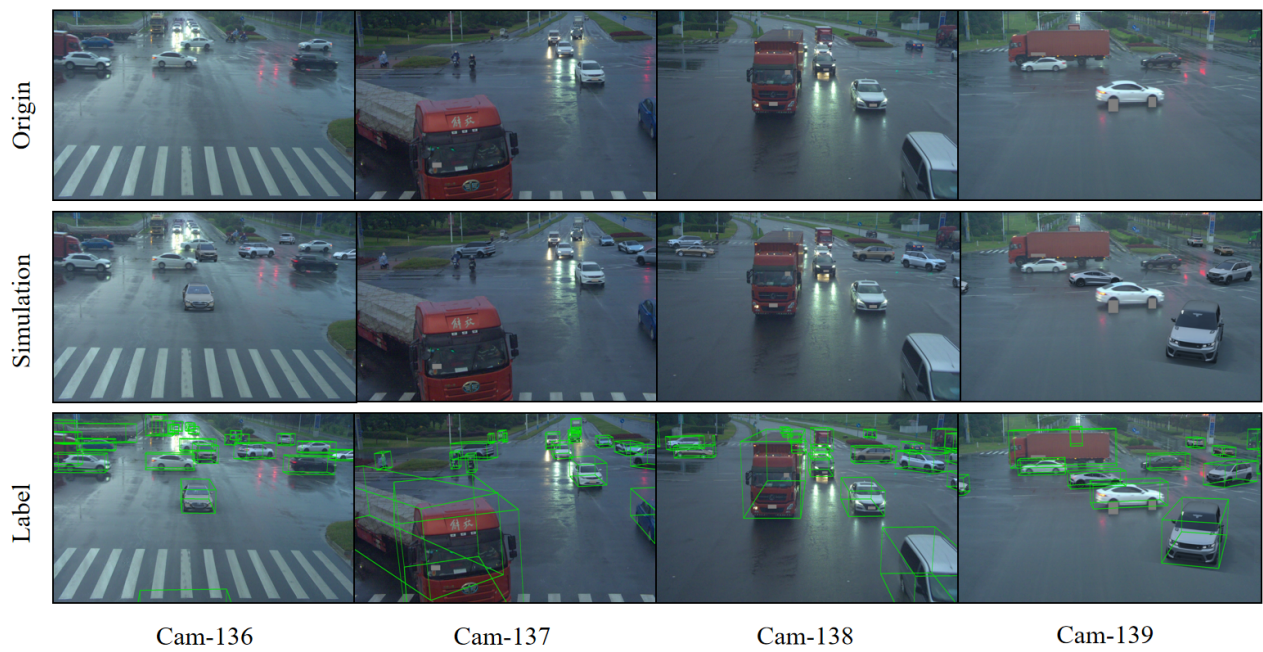


Figure 2. RoCo-Sim conducts multi-view simulation on Rcooper-136, and the simulation foreground has accurate 3D information.